IEEE Access
Multidisciplinary | Rapid Review | Open Access Journal

IEEE POWER & ENERGY SOCIETY SECTION

Received September 7, 2020, accepted September 22, 2020, date of publication September 29, 2020,
date of current version October 13, 2020.

Digital Object Identifier 10.1109/ACCESS.2020.3027699

DC Power Control Strategy of MMC for Commutation Failure Prevention in Hybrid Multi-Terminal HVDC System

CHOONGMAN LEE[1], (Graduate Student Member, IEEE), JAE WOONG SHIM[2], (Member, IEEE), HEEJIN KIM[1], (Member, IEEE), AND KYEON HUR[1], (Senior Member, IEEE)

[1]School of Electronic and Electrical Engineering, Yonsei University, Seoul 03722, South Korea
[2]Department of Energy Engineering, Inje University, Gimhae 50834, South Korea

Corresponding author: Kyeon Hur (khur@yonsei.ac.kr)

This work was supported in part by Korea Electric Power Corporation under Grant R17XA05-4, and in part by the Human Resources Program in Energy Technology of the Korea Institute of Energy Technology Evaluation and Planning (KETEP) Granted Financial Resource from the Ministry of Trade, Industry and Energy, South Korea under Grant 20194030202420.

ABSTRACT This article presents a control strategy for a modular multilevel converter (MMC) to prevent commutation failure of a line-commutated converter (LCC), forming a three-terminal hybrid HVDC transmission system, where one LCC sending end is connected to the large generation and two receiving ends (LCC inverter and MMC) are located near the load center. This configuration, one of the potential options, has been proposed to strengthen Korea electric power transmission system through the optimized use of existing assets and rights-of-way, extremely challenging to secure. The MMC power control strategy has been developed to regulate the AC voltage and the extinction angle of the LCC inverter. This indirect yet effective active and reactive power control of the LCC inverter terminal helps prevent the commutation failure (CF) of the LCC in emergency and maximize the benefits of the costly planning option. By establishing a theoretical foundation for this power control problem and relationship among the control parameters, we quantify the active power reference for MMC to secure the desired LCC extinction angle. A coordinated strategy has been developed for the AC filter, the on-load tap changer of a transformer, along with the MMC control to lower the risk of CF and its catastrophic impact on the whole power system. The validity and performance of the proposed control methods are demonstrated for the real Korea electric power planning cases using a real-time power system simulator.

INDEX TERMS Commutation failure, extinction angle, gamma-kick, hybrid multi-terminal HVDC system, weak AC system.

I. INTRODUCTION

In modern power systems, the line-commuted converter (LCC) high voltage DC (HVDC) system has been widely employed around the world for long-distance and bulk power transmission. Special attention has been paid to the LCC HVDC interface with weak AC systems, as LCC HVDC consumes massive reactive power when operating with high active power. The reactive power consumption of LCC HVDC may adversely affect AC voltage security [1]–[8]. In this case, where the LCC HVDC operates with large reactive power consumption and the grid is not strong enough to tightly regulate the AC voltage, the risk of commutation failure (CF) increases and threatens the whole system security [2]. In terms of CF, the increase of DC current and the decreased extinction angle may lead to CF due to the thyristor turn-off characteristics [2], and this CF can result in a shutdown of the LCC HVDC system and voltage instability on the AC-side [1]. Several indices for risk evaluation have been developed and reported to assess the stability of AC grids in the planning stage of LCC HVDC systems [9]–[16]. Besides, cascaded CF concerns were investigated for the large-scale multi-infeed HVDC systems [13].

To handle the CF, various solutions have been developed for the safe operation of LCC HVDC systems [17]–[30]. The voltage-dependent current-order limit strategies are

The associate editor coordinating the review of this manuscript and approving it for publication was Dragan Jovcic.

introduced to mitigate the CF by reducing the magnitude DC current [22]–[29]. In addition, the capacitor-commutated converter topology can be applied to prevent the CF [19]–[21]. In general, the method to increase the extinction angle is widely adapted for CF prevention [30]. This method commonly includes setting the minimum limit of the extinction angle for securing a margin and adjusting the on-load tap changer (OLTC) in a transformer for a high extinction angle.

These solutions are focused on increasing the extinction angle to mitigate the risk of CF; however, these solutions may inevitably face adverse impacts such as slow response time (slow switching behavior of AC filters and OLTC) or AC voltage drop which is caused by the consumption of reactive power from the LCC HVDC system [2]. Furthermore, the limitation of these solutions is that they may need to reduce the amount of power transmission considering the stability of AC grids. In this article, we thus present a method of controlling the extinction angle to mitigate the risk of CF without reducing power transmission to the load center.

A coordinated operation is developed among multiple HVDC lines called multi-infeed systems to improve the transmission capacity and system stability [9]–[12], [15], [16], [31], [32]. Recently, several utilities have carried out preliminary technical investigations to upgrade cos-effectively upgrade and exploit existing LCC HVDC systems, by tapping a new MMC station onto the LCC HVDC system, which is called a hybrid MTDC system [33]–[39]. The major advantage of this hybrid MTDC system is that it takes advantage of both LCC and MMC [40], resulting in a completely different set of characteristics than the LCC HVDC system itself due to the MMC terminal [33], i.e., the rapid and flexible operation and redirection [41]. This hybrid MTDC system can also be a cost-saving solution to large power transmission from a wind farm in a remote area compared to adding LCC HVDC lines for a multi-infeed HVDC system [33], [34]. The hybrid MTDC topology is considered to be feasible but practical issues including the DC fault remain to be further investigated for implementation. As adopted in this study, Full-bridge MMC with DC fault-blocking capability would be preferred [42], [43]. Studies for example, on the DC fault ride-through strategy and a proper fault clearing and recovery process for the hybrid MTDC system in [35] and the performance of the same hybrid MTDC topology for DC faults as presented in [44] should be beneficial and useful. These research efforts regarding the hybrid MTDC also have investigated the operation strategies, which however, do not directly address the critical CF problems.

This article thus proposes a strategy to mitigate the CF risk on the LCC inverter side using MMC power control in a hybrid MTDC structure, in cases where the MMC station is in the same area as the LCC inverter. Since the MMC is jointly connected with the LCC inverter on the AC and DC side, the MMC can flexibly control both the AC voltage drop and the DC current of the LCC inverter, implying control of the firing and extinction angle. The technical advantages and contributions of the proposed control scheme are summarized as follows.

- Regulating reactive power consumption by indirectly adjusting the active power of LCC inverter through the fast control of MMC
- Establishing a theoretical and practical framework for power flow control in the hybrid MTDC; a link between the extinction angle and DC power to the MMC, and an effective control scheme in emergency
- Lowering the risk of commutation failure and stabilizing the grid voltage and MTDC by coordinating the OLTC and the AC filters along with the MMC

The paper is organized as follows. Section II describes the background and operation of the topology. Section III introduces how to regulate the extinction angle and AC voltage through DC power control of MMC. In Section IV, the simulation results verify the efficacy of the proposed method.

II. HYBRID MULTI-TERMINAL HVDC

A. CONFIGURATION OF HYBRID MULTI-TERMINAL HVDC SYSTEM

Tapping a new MMC station onto the existing LCC HVDC system, the multi-terminal DC system is formed as shown in Fig. 1. In South Korea, the existing transmission network, including high voltage AC (HVAC) lines and LCC HVDC lines, delivers tremendous power from the East Coast area to massive load areas. HVAC lines and LCC HVDC lines are prepared to perform a ramp up/down operation in the contingency conditions of the network [45]. For instance, LCC HVDC lines immediately extend the transmission power amount when one of the HVAC lines is tripped. In addition, a Special Protection Scheme (SPS) has an important role to play in these conditions. Since the generators on the East Coast are critical to supplying the overall power demand of South Korea, the SPS is essential to prevent damage from the acceleration of these generators in case of a transmission network failure.

According to the announced Korean government's operation plan, a new nuclear power plant and thermal power plant will be added to the East Coast. As such, there is a growing need to enhance the transmission network for reliable power delivery. South Korea's transmission system operator (TSO) has pursued the construction of a new HVAC line. However, this project is suspended due to social responsibility issues. Instead, the installation of a new DC transmission system is currently ongoing.

As an encouraging solution, the MTDC topology is being prepared to improve the connectivity with existing HVDC lines and the flexibility of the network. Instead of building a new DC line, including two MMC stations, tapping an MMC onto the DC side is investigated to upgrade and exploit the existing LCC HVDC system cost-effectively. This topology features two receiving ends consisting of an LCC inverter and an MMC located in the load center. As such, the transmitted power from the LCC rectifier can be bypassed to the HVAC

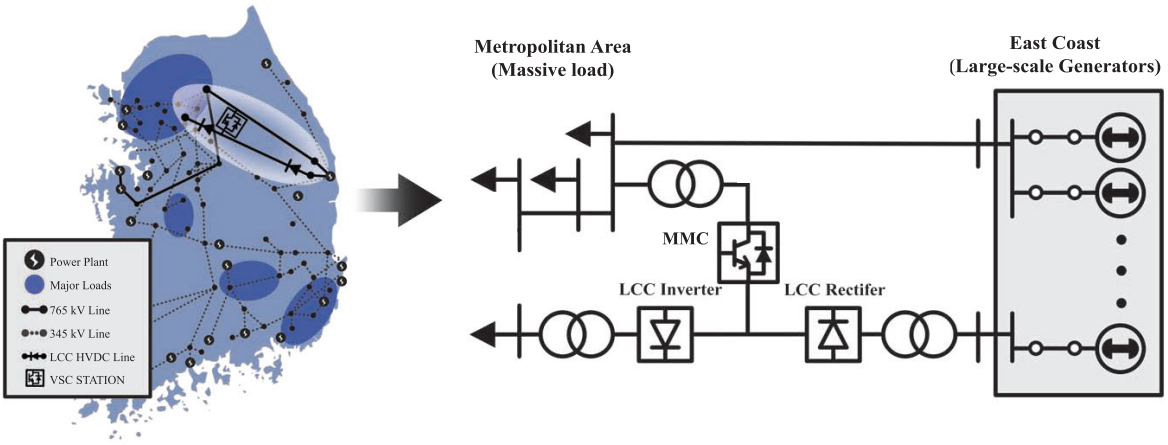

FIGURE 1. Transmission network structure of South Korea.

side through the bi-directional power flow capability of the MMC.

B. DC POWER FLOW OF HYBRID MULTI-TERMINAL HVDC SYSTEM

DC power flow in the hybrid MTDC is represented as follows:

$$P_{\text{demand}} = P_{\text{inv}} + P_{\text{mmc}} \tag{1}$$

where P_{demand} is the transmitted power from the LCC rectifier, P_{inv} is the absorbed power in the LCC inverter, and P_{mmc} is the absorbed power through the tapped MMC station.

As shown in Fig. 2, the LCC inverter and the MMC divide the power transmitted from the LCC rectifier as (1). The receiving power of the LCC inverter is defined as

$$P_{\text{inv}} = v_{\text{di}} i_{\text{di}}. \tag{2}$$

where $v_{\text{di}}(t)$ is the DC voltage, and $i_{\text{di}}(t)$ is the DC current of the LCC inverter.

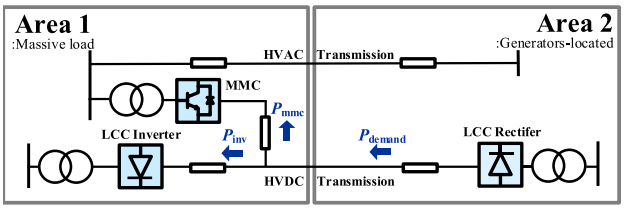

FIGURE 2. Simplified schematic of hybrid MTDC system.

Most importantly, if the power from the LCC rectifier P_{demand} is constant in (1), the higher power received through the MMC, the less power delivered to the LCC inverter. Accordingly, the DC power flow of MMC is then determined as follows:

$$\Delta P_{\text{mmc}} = \Delta P_{\text{inv}} \tag{3}$$

It should be noted that the amount of the receiving power of the LCC inverter affects the AC voltage drop and reactive power consumption on the LCC inverter side. Also, since the reactive power consumption in the LCC inverter varies depending on the extinction angle, the investigation is carried out considering the operating point of the LCC HVDC [46].

C. OPERATING POINT OF HYBRID MULTI-TERMINAL HVDC SYSTEM

Regarding the operation of the LCC HVDC system, the most common control mode of the LCC rectifier is a constant DC current (CC) mode and the DC voltage of the LCC rectifier is then determined as follows:

$$v_{\text{dr}}(t) = v_{\text{ac,r}} \cos\alpha(t) - I_{\text{dr}} R_{\text{cr}} \tag{4}$$

where $v_{\text{ac,r}}$ is the rectifier-side line-to-line AC voltage, $\alpha(t)$ is the ignition angle of LCC rectifier, R_{cr} is equivalent commutating resistance, and I_{dr} is the DC current reference for CC mode. The CC mode is illustrated as the gray line parallel to the y-axis as shown in Fig. 3.

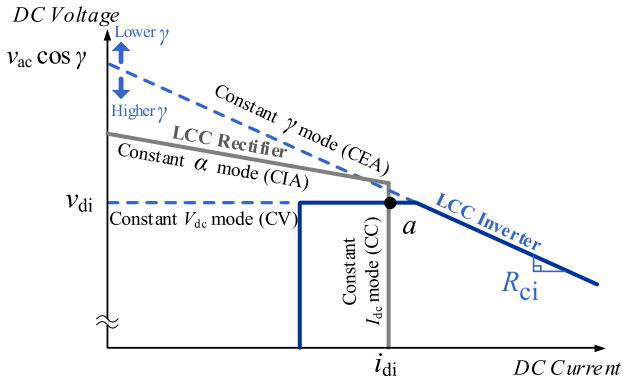

FIGURE 3. Operating point of LCC rectifier and inverter depending on control modes.

The second mode for LCC rectifier is to maintain the constant ignition angle (CIA):

$$v_{\text{dr}}(t) = v_{\text{ac,r}} \cos\alpha_{\text{a}} - i_{\text{dr}}(t) R_{\text{cr}} \tag{5}$$

where α_a is the reference ignition angle for LCC rectifier, and i_{dr} is DC current of LCC rectifier. The CIA mode is illustrated as the gray line with a slope in Fig. 3.

The most common control mode for LCC inverter is a constant DC voltage (CV) control and the DC voltage of the LCC inverter is obtained as follows [2], [6]:

$$v_{di}(t) = v_{ac}\cos\gamma(t) - i_d(t)R_{ci} \simeq V_{dc} \tag{6}$$

where v_{ac} is the inverter-side line-to-line AC voltage, $\gamma(t)$ is extinction angle, R_{ci} is equivalent commutating resistance, and V_{dc} is the DC voltage reference for CV mode.

Under CV mode, the extinction angle decreases as the DC current increases to regulate the DC voltage constantly. This mode is illustrated as the blue line parallel to the x-axis as shown in Fig. 3.

The second mode aims to maintain the constant extinction angle (CEA). Under the CEA mode, the DC voltage decreases as the DC current increases to regulate the extinction angle constantly as follows:

$$v_{di}(t) = v_{ac}\cos\gamma_a - i_{di}(t)R_{ci} \tag{7}$$

This mode is illustrated as the blue line with a slope in Fig. 3. As the extinction angle increases(or decreases), the CEA line moves downward(or upward). Consequently, the DC current flowing into the LCC inverter is defined as

$$i_{di}(t) = \frac{v_{ac}\cos\gamma(t) - v_{di}(t)}{R_{ci}}. \tag{8}$$

The CV mode is widely adopted among LCC HVDC operators. Note that the extinction angle increases as the DC current decreases under CV mode as manifested in (8). The DC current of LCC inverter thus decreases when the MMC delivers more power; the MMC can indirectly control the extinction angle.

Based on (2) and (3), the operating point of MMC is determined according to the DC current of LCC inverter in (8). The detailed MMC operating characteristics for implementing the proposed control are described in Section III.

III. PROPOSED EXTINCTION ANGLE AND AC VOLTAGE CONTROL METHOD

A. EXTINCTION ANGLE CONTROL

Regarding the risk of CF, a higher extinction angle can be a stable condition. The extinction angle can be extended as the DC current of the LCC decreases in (8). Based on (1) and (2), the DC power flow power control of the MMC can reduce the active power of the LCC inverter. In other words, with increased power through the MMC, the LCC inverter receives less DC current. Thus, the reduced DC current of the LCC inverter extends the extinction angle as (8). Consequently, we can obtain the margin of the extinction angle through the DC power flow control of the MMC. The reference for the extinction angle is as follows:

$$\gamma_{ref} = \gamma_{min} + \gamma_{margin} \tag{9}$$

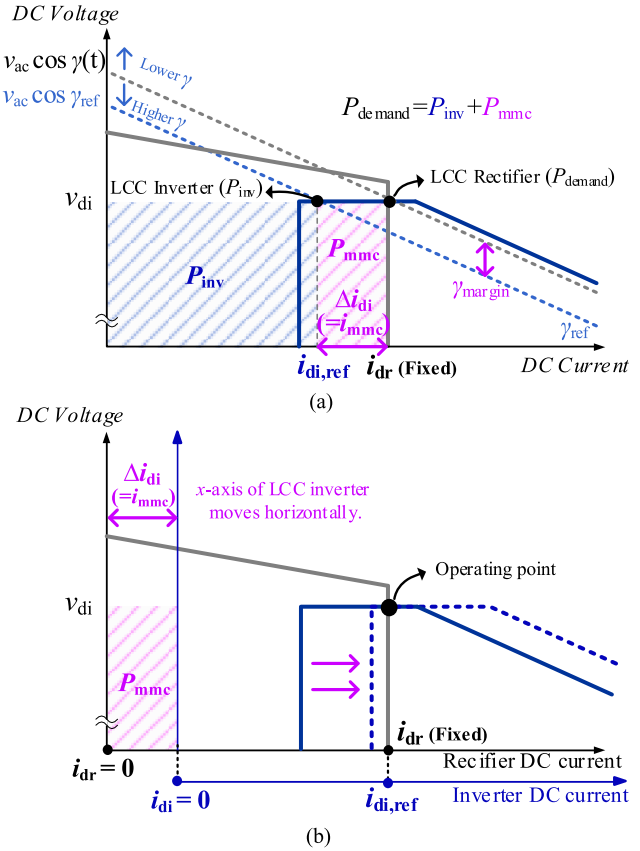

FIGURE 4. Diagrams for the operation of hybrid MTDC, (a) description of the proposed method through DC power control of MMC, and (b) determination of the operating point of hybrid MTDC system.

where γ_{ref} is the reference value for the extinction angle management, γ_{min} is the minimum extinction angle including the preset margin in consideration of AC disturbances, and γ_{margin} is the margin angle obtained by the proposed DC power control of MMC as shown in Fig. 4(a). Therefore, the DC current reference including (9) is

$$i_{di,ref} = \frac{v_{ac}\cos\gamma_{ref} - v_{di}}{R_{ci}}. \tag{10}$$

where $i_{di,ref}$ is the reference value for the DC current to control the extinction angle following the reference γ_{ref} including margin γ_{margin} in (9).

Combining (1) and (3), the receiving power and DC current of LCC inverter decreases, when MMC receives the power as much as ΔP_{mmc}. Therefore, the receiving power of the LCC inverter can be represented as a blue rectangle, and the receiving power of MMC can be represented as a purple rectangle as shown in Fig. 4(a).

Also, the extinction angle is controlled to γ_{ref} when DC current of LCC inverter is $i_{di,ref}$ as depicted in Fig. 4(a). As a consequence, the operating point of MMC can be obtained as follows:

$$\begin{aligned} P_{mmc} &= \Delta P_{inv} \\ &= v_{di}(i_{di,ref} - i_{di}(t)) \\ &= \frac{v_{di}v_{ac}}{R_{ci}}(\cos\gamma_{ref} - \cos\gamma(t)) \end{aligned} \tag{11}$$

We can quantify the active power order for the MMC to control the extinction angle to γ_{ref} including the margin γ_{margin}. Also, the operating point of LCC HVDC considering the proposed MMC power control can be determined by (10) and (11) as shown in Fig. 4(b). Note that the characteristic curve of the LCC inverter in Fig. 4(b) moves right along the x-axis as much as the MMC takes, and the intersection with the curve of the LCC rectifier becomes the operating point of the hybrid MTDC system.

B. MMC-ASSISTED GAMMA-KICK FUNCTION

This method can be applied during the AC filter switching. When a step-wise operation occurs in a capacitor bank of AC filters, an instantaneous fluctuation occurs on the extinction angle of the LCC inverter [47], [48]. For instance, when the steady-state AC voltage is higher than the rated value, a capacitor bank is turned off to lower the AC voltage. Following this, the AC voltage drops immediately at the moment of switching. The extinction angle can temporarily decrease below the minimum angle, which may lead to CF in severe cases.

For the undesired phenomenon, the conventional gamma-kick function averts the negative impact of the AC filter switching in advance [18]. The gamma-kick function pre-adjusts the extinction angle before switching to ensure that the angle remains in the normal range during the switching as shown in Fig. 5. This function should be coordinated with a well-planned sequence of the mechanical switching operations of AC filter and OLTC. Thorough investigation of communication delay and preparation time to ensure an exact process for safe switching should be required in practice. Before the AC filter switching, the receiving end power (LCC inverter power) decreases to adjust the extinction angle. After the AC filter switching, the receiving end power returns to the nominal operating point.

The limitations of the conventional gamma-kick function are that the power delivery from the sending end to the receiving end power must be reduced while the function is being performed and that the extinction angle is maintained near the minimum value with a higher risk of CF until the OLTC is operated as shown in Fig. 5.

Basically, the OLTC is activated to regulate the extinction angle. The discrete operation of the OLTC can be represented as $T(n)$ in the inverter-side line-to-line voltage $v_{\text{ac}}(t)$ as follows [3], [47]:

$$v_{\text{ac}}(t) = \frac{3\sqrt{2}}{\pi} BT(n)E_{\text{LL}} \tag{12}$$

where B is the number of bridges in the LCC inverter (a four-bridge converter is considered in this research), T(n) is the converter transformer tap ratio which depends on the discrete tap position n, and E_{LL} is the line-to-line voltage at the AC grid side.

In this research, the step size of the tap is 0.0125 with $\pm$ 16 gears, where the ratio ranges between 0.8 and 1.2 p.u.. The discrete tap position changes to maintain the extinction angle in the normal range with a certain dead-time.

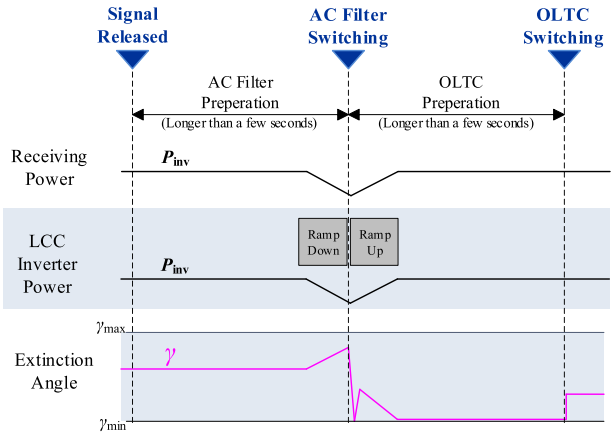

FIGURE 5. Diagram for the conventional gamma-kick function.

$$n = \begin{cases} n_0 + 1, & \gamma(t) < \gamma^{-}_{\text{normal}} \\ n_0, & \gamma^{-}_{\text{normal}} < \gamma(t) < \gamma^{+}_{\text{normal}} \\ n_0 - 1, & \gamma(t) > \gamma^{+}_{\text{normal}} \end{cases} \tag{13}$$

where n_0 is the previous position of the OLTC, $\gamma^{-}_{\text{normal}}$ and $\gamma^{+}_{\text{normal}}$ are the minimum and the maximum limit of the normal range, respectively.

$$v_{\text{di}} = \frac{3\sqrt{2}}{\pi} BT(n)E_{\text{LL}} \cos\gamma(t) - i_{\text{di}}R_{\text{ci}} \tag{14}$$

The extinction angle can be controlled by the adjustment of $T(n)$, which is the ratio of the OLTC in (12). However, the adjustment of the OLTC is also performed by the mechanical movement of gear. Thus, stress (including wear and tear) on the equipment is inevitable. Besides, since the operation delay time of the OLTC takes a few seconds, it cannot finely adjust the extinction angle immediately.

In this regard, we propose an MMC-assisted gamma-kick function based on the extinction control method utilizing the active power of MMC as (11). As shown in Fig. 6, it aims to

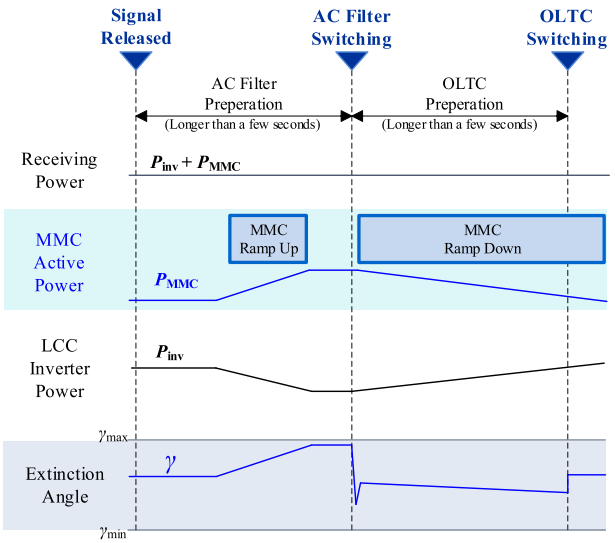

FIGURE 6. Diagram for the proposed MMC-assisted gamma-kick function.

pre-adjust the extinction angle before the AC filter switching through active power control of the MMC to prevent the transient phenomenon. After the AC filter switching and before the OLTC operation, which typically takes a few seconds, the MMC gradually reduces active power to maintain the extinction angle higher than the minimum angle and then returns to the nominal operating point as shown in Fig. 6. The proposed scheme does not compromise the desired power delivery. In addition, regulating the extinction angle in the normal range helps avoid unnecessary OLTC operations. The proposed MMC-assisted gamma-kick function thus helps coordinate operations among the AC filter, the OLTC, and the MMC control. Successful operation indeed depends on sufficiently fast and reliable communication and control architecture: upon detecting AC voltage variations, new orders for MMC and LCC are calculated and then dispatched simultaneously. For practical implementation, rigorous investigation beyond the scope of this article is required to synchronize the MMC and LCC in a complementary way.

C. AC VOLTAGE REGULATION

The reactive power consumption in LCC inverter is represented as follows [2]:

$$Q_{\text{inv}} = P_{\text{inv}} \tan\phi \tag{15}$$

$$\phi = \cos^{-1}\left(\frac{v_{\text{di}}}{v_{\text{ac}}}\right) \tag{16}$$

where Q_{inv} is the reactive power consumption in the LCC inverter, and ϕ is the power factor angle of the LCC inverter.

Based on these, the reactive power consumption of the LCC inverter is derived as follows:

$$Q_{\text{inv}} = P_{\text{inv}}\sqrt{\left(\frac{v_{\text{ac}}}{v_{\text{di}}}\right)^2 - 1}$$

$$= i_{\text{di}}\sqrt{{v_{\text{ac}}}^2 - {v_{\text{di}}}^2} \tag{17}$$

The proposed method can control the active power of LCC inverter through the power control of MMC, and accordingly, the reactive power of LCC inverter as (15) and (17). In other words, it indicates that the AC voltage of the LCC inverter-side can be regulated by controlling the active power of MMC with the proposed method.

Considering (3) and (17), the reactive power consumption in LCC inverter station can be represented as follows:

$$\Delta Q_{\text{inv}} = \Delta P_{\text{mmc}}\sqrt{\left(\frac{v_{\text{ac}}}{v_{\text{di}}}\right)^2 - 1} \tag{18}$$

It is noted that the reactive power of the LCC inverter can be regulated by DC power flow control through MMC as (18).

The DC current reference for LCC inverter is derived as follows based on (8):

$$\Delta i_{\text{di}}(t) = \frac{\Delta[v_{\text{ac}}(t)\cos\gamma(t)]}{R_{\text{ci}}} \tag{19}$$

Combining (2) and (19),

$$\Delta P_{\text{mmc}} = v_{\text{di}}\Delta i_{\text{di}}(t)$$

$$= K_{\text{p}}\Delta[v_{\text{ac}}(t)\cos\gamma(t)] \tag{20}$$

$$K_{\text{p}} = \frac{v_{\text{di}}}{R_{\text{ci}}} \tag{21}$$

where K_{p} is the proportional coefficient.

We present a control method that the AC voltage of the LCC inverter-side can be regulated by adjusting the active power of the MMC as (20). In order to verify the efficacy of the proposed method, we empirically obtain the steady-state relationship between the active power of the MMC and the AC voltage on the LCC inverter through repeated numerous simulations as shown in Fig. 7. Note that the AC filters' operation to compensate for the reactive power of the LCC inverter is disabled in order to investigate the effects of the DC power flow control of the MMC only.

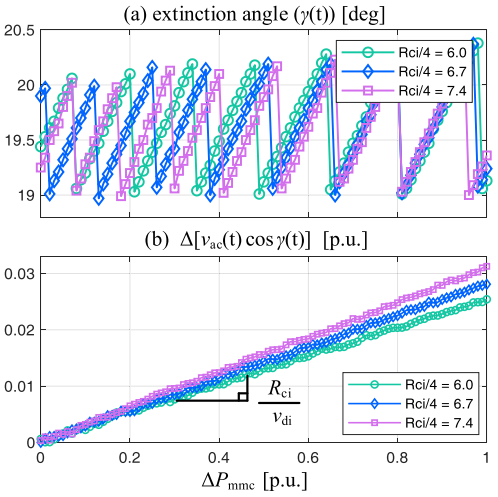

FIGURE 7. Steady-state operating points for the proposed control method. (a) extinction angle of LCC inverter. (b) inverter-side line-to-line voltage of LCC inverter and the cosine value of extinction angle.

As shown in Fig. 7(a), the extinction angle tends to increase as the active power of the MMC increases as (11); however, it cannot change linearly due to the discrete operation of the OLTC represented as $T(n)$ in (12). Note that the term multiplied by the line-to-line voltage of the inverter-side and the cosine function of the extinction angle responds linearly to the variation in the MMC active power as shown in Fig. 7(b). It should also be noted that the slope of the lines in Fig. 7(b) is determined by K_{p} in (21). Therefore, the magnitude of AC voltage varies depending on the R_{ci} pre-determined by the reactance component of the AC network and converter transformers. Accordingly, it is shown that the proportional control by DC power control of the MMC can be applied to this hybrid MTDC system as (20) and (21).

Comprehensively, the relationship between MMC active power, extinction angle, and AC voltage of the LCC-inverter side is shown in Fig. 8. It is verified that as the active power of

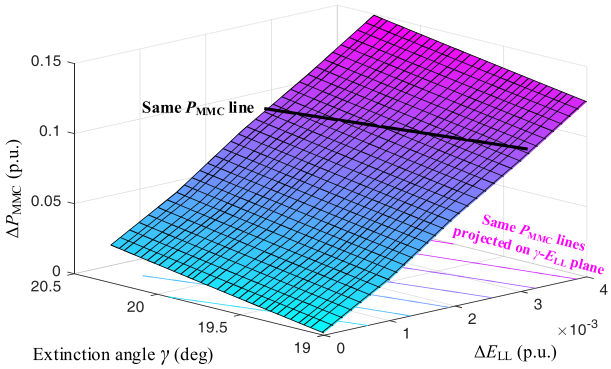

FIGURE 8. Relationship between MMC active power, extinction angle, and AC voltage of the LCC-inverter side.

MMC increases, the extinction angle and AC voltage of LCC inverter-side can increase.

Since the deviation of the cosine value of the extinction angle is negligible compared to the magnitude of the AC voltage in (20), the proportional controller can be designed as follows:

$$\Delta P_{\mathrm{mmc}}{}^{*} = K_{\mathrm{p}}[v_{\mathrm{ac}}{}^{*} - v_{\mathrm{ac}}(t)] \tag{22}$$

where v_{ac}^{*} is the reference for the inverter-side line-to-line voltage.

Including (11) and (20), the overall control system for the MMC can be designed as shown in Fig. 9. The active power control loop of the MMC can be composed of the extinction angle control and remote (LCC inverter side) AC voltage control. The proposed MMC-assisted gamma-kick function described in Fig. 6 will be performed at the operators' option.

It is worth noting that the active power of the MMC should be coordinated with the LCC HVDC system, not to be faster than the response of the LCC HVDC system. This limit is predetermined in the planning stage according to the national reliability performance standards, particularly to ensure the transient stability of the whole system. Therefore, the rate of change of active power is

$$\frac{\Delta P_{\mathrm{mmc}}}{\Delta t} < \frac{\Delta P_{\mathrm{LCC}}}{\Delta t}. \tag{23}$$

where $\Delta P_{\mathrm{LCC}}/\Delta t$ is the rate of change of active power of the existing LCC HVDC system.

In addition, since the rated capacity of the LCC HVDC system and the MMC are not identical in this research, hard limiters are needed in the current control unit as follows:

$$i_{\mathrm{d,ref}} = \begin{cases} i_{\mathrm{di,min}}, & i_{\mathrm{d,ref}} < i_{\mathrm{di.min}} \\ \dfrac{\Delta P_{\mathrm{mmc}}}{v_{\mathrm{di}}}, & i_{\mathrm{di,min}} < i_{\mathrm{d,ref}} < i_{\mathrm{di.max}} \\ i_{\mathrm{di,max}}, & i_{\mathrm{d,ref}} > i_{\mathrm{di.max}} \end{cases} \tag{24}$$

where $i_{\mathrm{d,ref}}$ is the reference for d-axis current of the MMC controller, $i_{\mathrm{di,min}}$ and $i_{\mathrm{di,max}}$ are the minimum and maximum current limit of the LCC inverter, respectively.

The reactive power control loop, local AC voltage control loop, and the inner controller are set identically with the existing control system of the MMC as shown in Fig. 9.

TABLE 1. Parameters of Hybrid MTDC System and AC Network.

Parameters	LCC Rectifier	LCC Inverter	MMC
Rated capacity (MVA)	4000	4000	1000
Rated DC voltage (kV)	500	500	500
Transformer ratio (kV)	345/214	345/211	345/300
Leakage reactance (pu)	0.18	0.18	0.10
No. of six-pulse bridge B	4	4	–
No. of submodules per arm	–	–	512
Short-circuit ratio	7	4	4
X/R ratio	8	10	10
Equivalent commutating resistance per bridge $R_{\mathrm{c}}/4$ (Ω)	6.4	6.7	–
Firing angle limit (deg)	$\alpha_{\min} = 2$	$\gamma_{\min} = 17$	–
Control mode	DC current control	DC voltage control	DC current control

IV. SIMULATION RESULTS

A. COMMUTATION FAILURE PREVENTION

This section demonstrates the effect of the proposed method in the hybrid MTDC system using a real-time power system simulator. The system parameters are summarized in Table 1. To verify the effect of mitigating CF, we evaluate the hybrid MTDC system with the proposed method through two indices. Commutation failure immunity index (CFII) is an indicator of how robust the system is against CF [15], [16]. CFII is represented as follows:

$$\mathrm{CFII} = \left(\frac{{E_{\mathrm{LL}}}^{2}}{Z_{\mathrm{fault}} \cdot P_{\mathrm{dc}}}\right) \cdot 100. \tag{25}$$

where Z_{fault} is the fault impedance, and P_{dc} is the rated DC power.

It indicates that the larger the CFII, the more robust against CF. The CF mitigation effect of the proposed method is verified by comparing the CFII of the hybrid MTDC system. For the three-phase resistive fault, CFII of the hybrid MTDC with the proposed method is higher than that without the method as shown in Fig. 10. Based on (22), the proposed method indirectly regulates the AC voltage of LCC inverter-side through DC power control of MMC. Therefore, it is confirmed that the hybrid MTDC system becomes more robust against CF through the proposed method.

Critical voltage drop (CVD) is another indicator to represent the maximum AC voltage drop without CF. In other words, CVD is the maximum allowable voltage drop (three-phase) that does not cause the CF. In this research, the CVD values are obtained through numerous simulations by causing the AC voltage reduction at different points on waves, similarly to [15], [16], [49], [50]. The CF occurs on a voltage drop that is more severe than CVD. Therefore, the operating point where the AC voltage drop is more critical than CVD is in the commutation failure region as shown in Fig. 11. Most importantly, as the active power of MMC increases, the CVD increases, and the safe region can be extended. Besides, it is noted that the higher the short-circuit ratio (SCR), the larger the CVD.

A dynamic simulation is performed to demonstrate the CF mitigation effect of the proposed method using a real-time power system simulator. Fig. 12 shows the response of hybrid

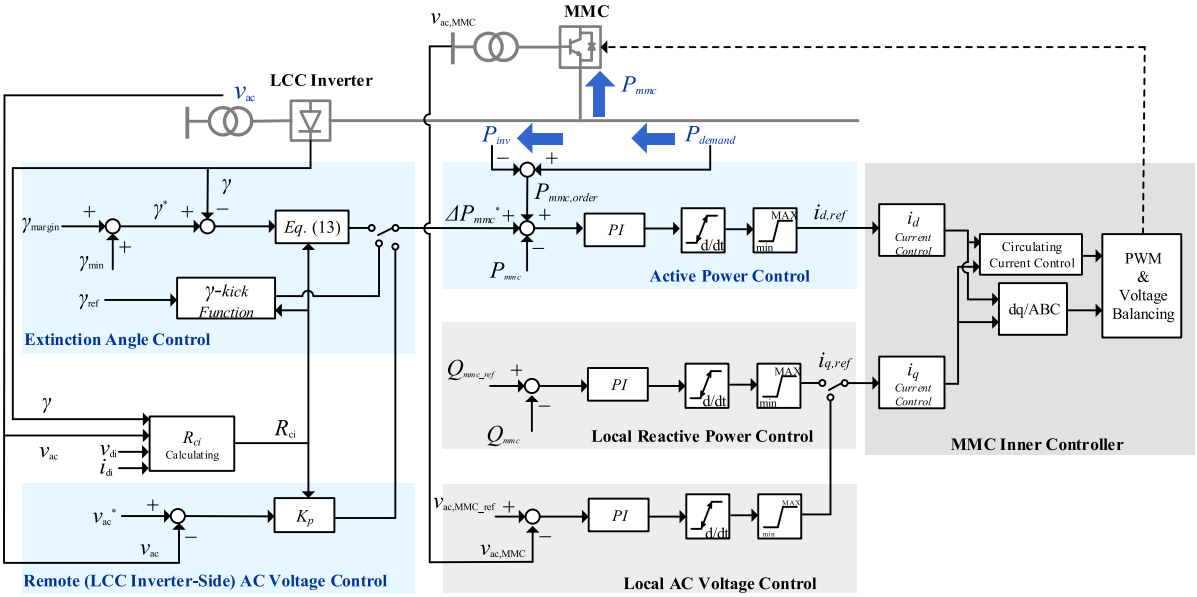

FIGURE 9. The overall control diagram of the proposed method for MMC within hybrid multi-terminal DC.

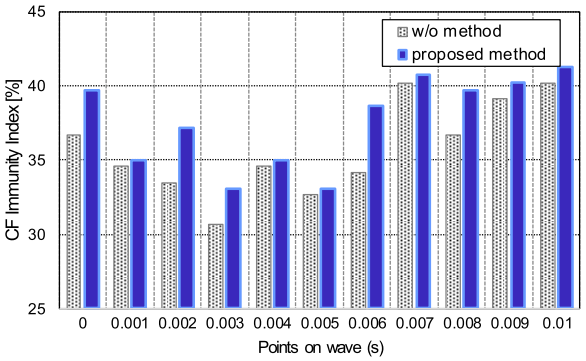

FIGURE 10. Commutation Failure Immunity Index (CFII) for the hybrid MTDC system with and without proposed method.

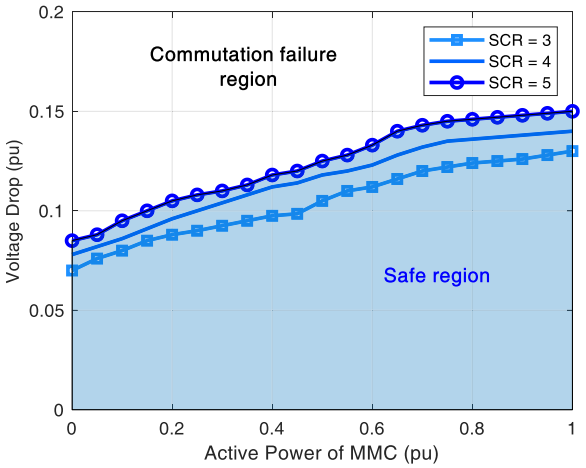

FIGURE 11. Critical voltage drop (CVD) curves according to short circuit ratio.

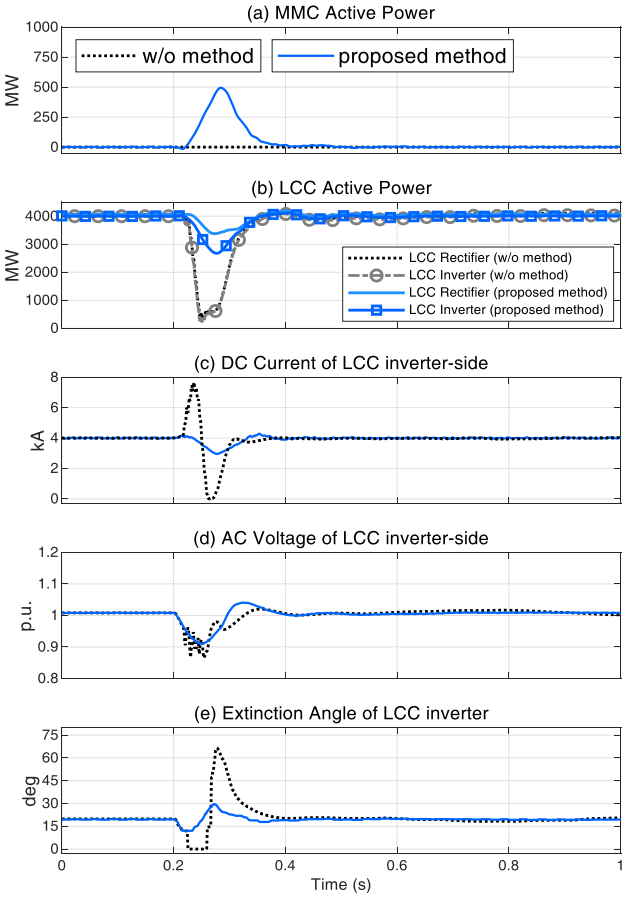

FIGURE 12. System responses with and without the proposed method according to the AC voltage drop at 0.2 s (the case without the proposed method faced commutation failure only).

MTDC when an AC voltage drop of 0.1 p.u. occurs at the instance of 0.2 s and is cleared after five cycles. When the proposed method is not utilized, CF occurs as indicated by the dotted line in Fig. 12. Under the proposed method, the hybrid MTDC system can avoid the CF by increasing the active power of MMC according to the AC voltage drop and simultaneously reducing the active power and DC current of the LCC inverter. Fig. 13 shows the results of the dynamic

simulation in Fig. 12 simultaneously with the CVD curve (when the SCR is 4) in Fig. 11. Without the proposed method, the operating point reaches the commutation failure region as shown in Fig. 13. On the other hand, the proposed method increases the active power through MMC and consequently allows the operating point to remain in the safe region. Therefore, the dynamic simulation results in Fig. 12 correspond with the analysis in Fig. 13, which simultaneously shows that CF can be avoided through the proposed method.

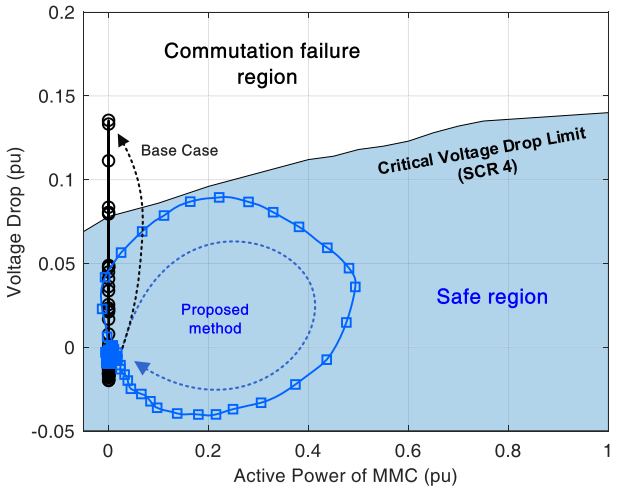

FIGURE 13. Critical voltage drop curve (SCR 4 in Fig. 11) and the traces of MMC power(Fig. 12(a))-Voltage drop(Fig. 12(d)) for the base case (black line) and the proposed method (blue-line).

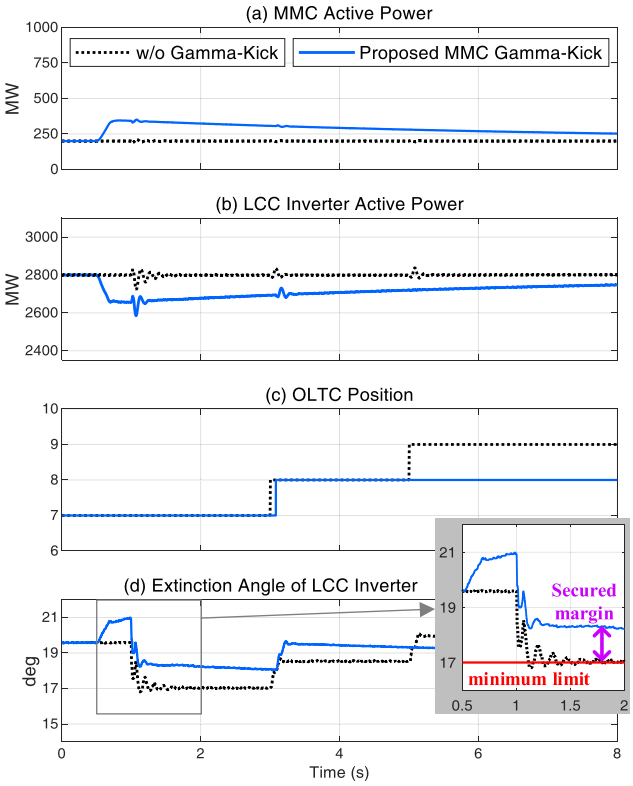

FIGURE 14. System responses with and without the proposed MMC-assisted gamma-kick function according to AC filter switching at 1.0 s.

B. MMC-ASSISTED GAMMA-KICK FOR AC FILTER SWITCHING

This section demonstrates the application of the proposed MMC-assisted gamma-kick function in the hybrid MTDC system. Two AC filter switching cases to regulate AC voltage under normal operating condition are investigated using a real-time power system simulator. Fig. 6 shows the principle of the proposed MMC-kick function based on (11) and (14). Note that the 34 Mvar capacitor bank in the AC filters is turned out at the instant of 1 s as shown in Fig. 14.

Without the proposed MMC-assisted gamma-kick function, switching in a capacitor bank caused an undesired oscillation on the extinction angle of the LCC inverter as shown in Fig. 14(d). The extinction angle immediately decreases below the minimum angle value of 17°. In addition, the number of operating cycles of the OLTC is two to regulate the extinction angle within the normal range after the AC filter switching as shown in Fig. 14(c). Note that the OLTC operation takes more than a few seconds, though we assume it takes two seconds in this section.

On the other hand, the proposed MMC-assisted gamma-kick function can prevent unnecessary transients when switching AC filters. Before turning off a capacitor bank, the extinction angle is pre-adjusted to 21° through the active power control of the MMC to ensure the safe commutation of the LCC inverter during the AC filter switching. Based on (11), the power order for regulating the extinction angle to 21° is calculated to be 343 MW. Furthermore, the number of OLTC switchings is reduced from two to one as shown in Fig. 14(c) with the proposed function. It is confirmed that this reduces the mechanical stress on the OLTC, supporting stable LCC HVDC system operation.

C. GENERATOR TRIP

When a 100 MW generator near the LCC inverter area is tripped, the impact on AC voltage regulation of the proposed method is investigated. After the generator is tripped (at 0.5 s), a significant fluctuation occurs in the AC voltage on the LCC inverter's side as given in Fig. 15(c). The extinction angle also falls below the minimum angle as shown in Fig. 15(d). Also, the fluctuation of the extinction angle also causes undesired transients in the active power transfer as shown in Fig. 15(b).

On the other hand, the proposed control method prevents unnecessary transients when the generator is tripped. The proposed method immediately adjusts the active power of the MMC depending on the AC voltage deviation according to (22). As a result, the oscillation of the AC voltage of the LCC inverter is attenuated as shown in Fig. 15(c) and the deviation of extinction angle are alleviated as shown in Fig. 15(d). The extinction angle remains within the normal range, in contrast to the response without the proposed method where the angle drops below the minimum angle.

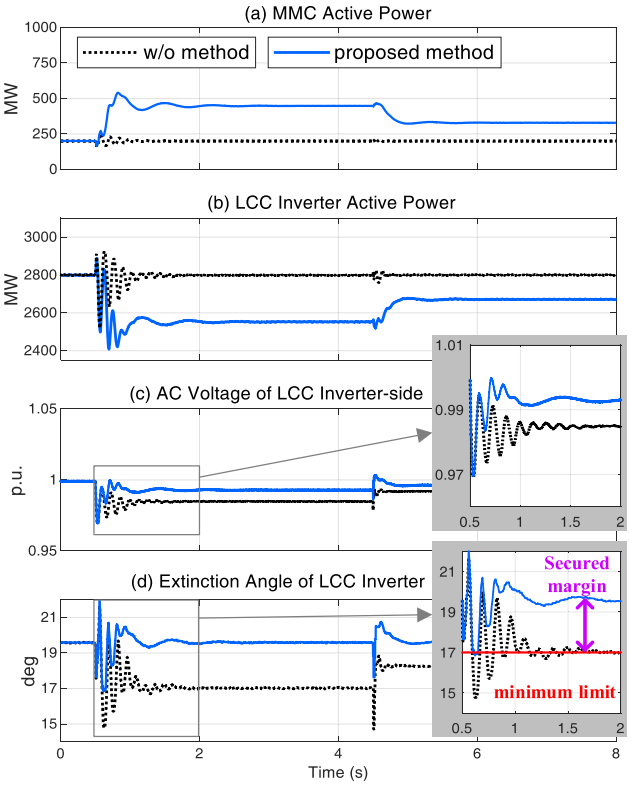

FIGURE 15. System responses with and without the proposed method according to a generator tripping at 0.5s.

V. CONCLUSION

As a potential option to enhance the transmission network in Korea, tapping an MMC station onto an existing LCC HVDC system creates a hybrid MTDC system. While offering flexibility in controlling power flows via the MMC, the hybrid MTDC still has the same reactive power and the AC voltage stability concerns on the LCC inverter, possibly causing the commutation failure (CF). To reduce the risk of CF and ensure the safe operation of the LCC inverter, this article presents the MMC power flow control to regulate the extinction angle of the LCC inverter and the AC voltage under contingency conditions. As demonstrated through the rigorous simulation studies, the proposed control strategy can significantly improve the CF immunity, and the MMC-assisted gamma-kick helps perform harmoniously with the AC filter and the OLTC operations. Findings through this study should be beneficial for ongoing and future hybrid MTDC projects.

REFERENCES

[1] B. Franken and G. Andersson, "Analysis of HVDC converters connected to weak AC systems," *IEEE Trans. Power Syst.*, vol. 5, no. 1, pp. 235–242, Feb. 1990.

[2] P. Kundur, *Power System Stability and Control* (The EPRI Power System Engineering Series). New York, NY, USA: McGraw-Hill, 1994.

[3] G.-S. Lee, D.-H. Kwon, S.-I. Moon, and P.-I. Hwang, "Reactive power control method for the LCC rectifier side of a hybrid HVDC system exploiting DC voltage adjustment and switched shunt device control," *IEEE Trans. Power Del.*, vol. 35, no. 3, pp. 1575–1587, Jun. 2020.

[4] Y. Li, L. Luo, C. Rehtanz, S. Rüberg, and F. Liu, "Realization of reactive power compensation near the LCC-HVDC converter bridges by means of an inductive filtering method," *IEEE Trans. Power Electron.*, vol. 27, no. 9, pp. 3908–3923, Sep. 2012.

[5] Y. Xue and X.-P. Zhang, "Reactive power and AC voltage control of LCC HVDC system with controllable capacitors," *IEEE Trans. Power Syst.*, vol. 32, no. 1, pp. 753–764, Jan. 2017.

[6] A. Hammad, K. Sadek, H. Koelsch, and G. Gueth, "Advanced scheme for AC voltage control at HVDC converter terminals," *IEEE Trans. Power App. Syst.*, vol. PAS-104, no. 3, pp. 697–703, Mar. 1985.

[7] K. W. Kanngiesser and H. P. Lips, "Control methods for improving the reactive power characteristic of HVDC links," *IEEE Trans. Power App. Syst.*, vol. PAS-89, no. 6, pp. 1120–1125, Jul. 1970.

[8] N. A. Vovos and G. D. Galanos, "Damping of power swings in AC tie lines using a parallel DC link operating at constant reactive power control," *IEEE Trans. Power App. Syst.*, vol. PAS-98, no. 2, pp. 416–425, Mar. 1979.

[9] Y. Liu and Z. Chen, "A flexible power control method of VSC-HVDC link for the enhancement of effective short-circuit ratio in a hybrid multi-infeed HVDC system," *IEEE Trans. Power Syst.*, vol. 28, no. 2, pp. 1568–1581, May 2013.

[10] C. Xia, X. Hua, Z. Wang, and Z. Huang, "Analytical calculation for multi-infeed interaction factors considering control modes of high voltage direct current links," *Energies*, vol. 11, no. 6, p. 1506, Jun. 2018.

[11] D. L. H. Aik and G. Andersson, "Voltage stability analysis of multi-infeed HVDC systems," *IEEE Trans. Power Del.*, vol. 12, no. 3, pp. 1309–1318, Jul. 1997.

[12] D. L. H. Aik and G. Andersson, "Analysis of voltage and power interactions in multi-infeed HVDC systems," *IEEE Trans. Power Del.*, vol. 28, no. 2, pp. 816–824, Apr. 2013.

[13] J. Xu, T. Lan, S. Liao, Y. Sun, D. Ke, X. Li, J. Yang, and X. Peng, "An on-line power/voltage stability index for multi-infeed HVDC systems," *J. Mod. Power Syst. Clean Energy*, vol. 7, no. 5, pp. 1094–1104, Sep. 2019.

[14] Y. Shao and Y. Tang, "Fast evaluation of commutation failure risk in multi-infeed HVDC systems," *IEEE Trans. Power Syst.*, vol. 33, no. 1, pp. 646–653, Jan. 2018.

[15] E. Rahimi, A. M. Gole, J. B. Davies, I. T. Fernando, and K. L. Kent, "Commutation failure in single-and multi-infeed HVDC systems," in *Proc. 8th IEE Int. Conf. AC DC Power Transmiss. (ACDC)*, Mar. 2006, pp. 182–186.

[16] Z. Wei, J. Liu, W. Fang, J. Hou, and Z. Xiang, "Commutation failure analysis in single-and multi-infeed HVDC systems," in *Proc. IEEE PES Asia–Pacific Power Energy Eng. Conf. (APPEEC)*, Oct. 2016, pp. 2244–2249.

[17] B. Davies *et al.*, "Systems with multiple DC infeed," in *Proc. CIGRE Working Group B4. 41*, Dec. 2008.

[18] L. Cheng, Z. Zhang, S. Niu, X. Ke, and T. Huo, "Modeling of reactive power control system of HVDC," in *Proc. Asia–Pacific Power Energy Eng. Conf.*, Mar. 2010, pp. 1–4.

[19] S. Gomes, N. Martins, T. Jonsson, D. Menzies, and R. Ljungqvist, "Modeling capacitor comnmutated converters in power system stability studies," *IEEE Power Eng. Rev.*, vol. 22, no. 4, p. 76, Apr. 2002.

[20] K. Sadek, M. Pereira, D. P. Brandt, A. M. Gole, and A. Daneshpooy, "Capacitor commutated converter circuit configurations for DC transmission," *IEEE Trans. Power Del.*, vol. 13, no. 4, pp. 1257–1264, Oct. 1998.

[21] Z. Siyu, L. Sizhuo, C. Wenjia, Y. Wei-yang, and W. Jun, "Study on transient characteristics of CCC-HVDC transmission systems," in *Proc. Int. Conf. Sustain. Power Gener. Supply (SUPERGEN)*, 2012, pp. 1–5.

[22] R. Bunch and D. Kosterev, "Design and implementation of AC voltage dependent current order limiter at pacific HVDC intertie," *IEEE Trans. Power Del.*, vol. 15, no. 1, pp. 293–299, Jan. 2000.

[23] C. W. Taylor and S. Lefebvre, "HVDC controls for system dynamic performance," *IEEE Trans. Power Syst.*, vol. 6, no. 2, pp. 743–752, May 1991.

[24] F. Karlecik-Maier, "A new closed loop control method for HVDC transmission," *IEEE Trans. Power Del.*, vol. 11, no. 4, pp. 1955–1960, Oct. 1996.

[25] M. Jafar and M. Molinas, "Effects and mitigation of post-fault commutation failures in line-commutated HVDC transmission system," in *Proc. IEEE Int. Symp. Ind. Electron.*, Jul. 2009, pp. 81–85.

[26] M. O. Faruque, Y. Zhang, and V. Dinavahi, "Detailed modeling of CIGRÉ HVDC benchmark system using PSCAD/EMTDC and PSB/SIMULINK," *IEEE Trans. Power Del.*, vol. 21, no. 1, pp. 378–387, Jan. 2006.

[27] Z. Wei, Y. Yuan, X. Lei, H. Wang, G. Sun, and Y. Sun, "Direct-current predictive control strategy for inhibiting commutation failure in HVDC converter," *IEEE Trans. Power Syst.*, vol. 29, no. 5, pp. 2409–2417, Sep. 2014.

[28] D. Shu, Q. Jiang, C. Zhang, Z. Liu, and C. Li, "Improved current order control strategy for effective mitigation of commutation failure in HVDC system," in *Proc. IEEE Power Energy Soc. Gen. Meeting*, Jul. 2017, pp. 1–5.
[29] C. Guo, Y. Liu, C. Zhao, X. Wei, and W. Xu, "Power component fault detection method and improved current order limiter control for commutation failure mitigation in HVDC," *IEEE Trans. Power Del.*, vol. 30, no. 3, pp. 1585–1593, Jun. 2015.
[30] Y. Z. Sun, L. Peng, F. Ma, G. J. Li, and P. F. Lv, "Design a fuzzy controller to minimize the effect of HVDC commutation failure on power system," *IEEE Trans. Power Syst.*, vol. 23, no. 1, pp. 100–107, Feb. 2008.
[31] C. Zhang, X. Chu, B. Zhang, L. Ma, X. Li, X. Wang, L. Wang, and C. Wu, "A coordinated DC power support strategy for multi-infeed HVDC systems," *Energies*, vol. 11, no. 7, p. 1637, Jun. 2018. [Online]. Available: https://www.mdpi.com/1996-1073/11/7/1637
[32] Y. Liu and Z. Chen, "Power control method on VSC-HVDC in a hybrid multi-infeed HVDC system," in *Proc. IEEE Power Energy Soc. Gen. Meeting*, Jul. 2012, pp. 1–8.
[33] X. Chen, H. Sun, J. Wen, W.-J. Lee, X. Yuan, N. Li, and L. Yao, "Integrating wind farm to the grid using hybrid multiterminal HVDC technology," *IEEE Trans. Ind. Appl.*, vol. 47, no. 2, pp. 965–972, Mar. 2011.
[34] M. H. Nguyen, T. K. Saha, and M. Eghbal, "Hybrid multi-terminal LCC HVDC with a VSC converter: A case study of simplified South East Australian system," in *Proc. IEEE Power Energy Soc. Gen. Meeting*, Jul. 2012, pp. 1–8.
[35] N. M. Haleem, A. D. Rajapakse, A. M. Gole, and I. T. Fernando, "Investigation of fault ride-through capability of hybrid VSC-LCC multi-terminal HVDC transmission systems," *IEEE Trans. Power Del.*, vol. 34, no. 1, pp. 241–250, Feb. 2019.
[36] Y. Liu, L. Zhang, and H. Liang, "DC voltage adaptive droop control strategy for a hybrid multi-terminal HVDC system," *Energies*, vol. 12, no. 3, p. 380, Jan. 2019.
[37] S. Hwang, S. Song, G. Jang, and M. Yoon, "An operation strategy of the hybrid multi-terminal HVDC for contingency," *Energies*, vol. 12, no. 11, p. 2042, May 2019. [Online]. Available: https://www.mdpi.com/1996-1073/12/11/2042
[38] M. H. Nguyen, T. K. Saha, and M. Eghbal, "Master self-tuning VDCOL function for hybrid multi-terminal HVDC connecting renewable resources to a large power system," *IET Gener., Transmiss. Distrib.*, vol. 11, no. 13, pp. 3341–3349, Sep. 2017.
[39] B. Li, Y. Liang, G. Wang, H. Li, and X. Chen, "A control parameter design method for hybrid multi-terminal HVDC system," *IEEE Access*, vol. 8, pp. 18669–18680, 2020.
[40] R. E. Torres-Olguin, M. Molinas, and T. Undeland, "Offshore wind farm grid integration by VSC technology with LCC-based HVDC transmission," *IEEE Trans. Sustain. Energy*, vol. 3, no. 4, pp. 899–907, Oct. 2012.
[41] K. Sharifabadi, L. Harnefors, H.-P. Nee, S. Norrga, and R. Teodorescu, *Design, Control, and Application of Modular Multilevel Converters for HVDC Transmission Systems*. Hoboken, NJ, USA: Wiley, 2016.
[42] N. R. Chaudhuri, B. Chaudhuri, R. Majumder, and A. Yazdani, *Multiterminal Direct-Current Grids: Modeling, Analysis, and Control*. Hoboken, NJ, USA: Wiley, 2014.
[43] D. Jovcic and K. H. Ahmed, *High Voltage Direct Current Transmission: Converters, Systems and DC Grids*. Hoboken, NJ, USA: Wiley, 2015.
[44] D. H. R. Suriyaarachchi, C. Karawita, and M. Mohaddes, "Applicability of full-bridge and half-bridge MMC for tapping LCC HVDC," in *Proc. 13th IET Int. Conf. AC DC Power Transmiss. (ACDC)*, 2017, pp. 1–6.
[45] T. Machida, "Improving transient stability of AC system by joint usage of DC system," *IEEE Trans. Power App. Syst.*, vol. PAS-85, no. 3, pp. 226–232, Mar. 1966.
[46] A. Zheng, C. Guo, P. Cui, W. Jiang, and C. Zhao, "Comparative study on small-signal stability of LCC-HVDC system with different control strategies at the inverter station," *IEEE Access*, vol. 7, pp. 34946–34953, 2019.
[47] J. C. Das, "Analysis and control of large-shunt-capacitor-bank switching transients," *IEEE Trans. Ind. Appl.*, vol. 41, no. 6, pp. 1444–1451, Nov. 2005.
[48] M. Liu, L. Zheng, F. Shi, and K. Li, "Commutation failure caused by AC filter switching in HVDC system," *J. Eng.*, vol. 2019, no. 16, pp. 889–892, Mar. 2019.
[49] J. Zhang, Y. Li, J. Song, X. Chen, and Y. Zhang, "Calculation method of critical voltage drop of DC commutation process considering AC system three-phase fault moments," *J. Eng.*, vol. 2019, no. 16, pp. 1630–1635, Mar. 2019.
[50] C. V. Thio, J. B. Davies, and K. L. Kent, "Commutation failures in HVDC transmission systems," *IEEE Trans. Power Del.*, vol. 11, no. 2, pp. 946–957, Apr. 1996.

CHOONGMAN LEE (Graduate Student Member, IEEE) received the B.S. degree in electrical engineering from Myongji University, Seoul, South Korea, in 2013. He is currently pursuing the M.S./Ph.D. degrees in electrical engineering with Yonsei University, Seoul. His research interests include modeling and control of power converters, power electronic applications in power systems, and integration of renewable energy.

JAE WOONG SHIM (Member, IEEE) received the Ph.D. degrees in electrical engineering jointly from Yonsei University, Seoul, South Korea, and The University of Sydney, Sydney, NSW, Australia, in 2016. He was a Senior Researcher with the HVDC Research Center, LS Electric Company Ltd., from 2016 to 2017, for HVDC/FACTS operation and control. Since 2017, he has been with the Department of Energy Engineering, Inje University, South Korea, where he is currently leading the Electric Power System Laboratory. His research interests include power system dynamics and control, HVDC/FACTS/MTDC/MVDC/ESS operation and control, wide-area control with renewable energy sources, and the power system stability issues with power electronics devices.

HEEJIN KIM (Member, IEEE) received the B.S. and Ph.D. degrees in electrical engineering from Yonsei University, Seoul, South Korea, in 2010 and 2015, respectively. He was a Postdoctoral Fellow with Yonsei University, from 2015 to 2019. Since 2019, he has been with Yonsei University as a Research Professor. His research interests include modeling and control of power converters, modular multilevel converters, flexible ac transmission systems/high-voltage direct current, power electronic applications in power systems, and integration of renewable energy.

KYEON HUR (Senior Member, IEEE) received the B.S. and M.S. degrees in electrical engineering from Yonsei University, Seoul, South Korea, in 1996 and 1998, respectively, and the Ph.D. degree in electrical and computer engineering from The University of Texas at Austin, Austin, TX, USA, in 2007. He was a Research and Development Engineer with Samsung Electronics, Suwon, South Korea, from 1998 to 2003. His industrial experience includes Electric Reliability Council of Texas, Taylor, TX, USA, as a Grid Operations Engineer, from 2007 to 2008. He was also with the Electric Power Research Institute, Palo Alto, CA, USA, and conducted and managed research projects in grid operations and planning, from 2008 to 2010. He rejoined Yonsei University, in 2010, and since 2010, has been leading the Smart-Grid Research Group. His current research interests include flexible ac transmission systems/high-voltage direct current, power system dynamics and control, and integration of variable generation and controllable load.